Appl. Math. Mech. -Engl. Ed., **34**(9), 1145–1154 (2013)
DOI 10.1007/s10483-013-1733-7

Applied Mathematics and Mechanics (English Edition)

Nonlinear progressive damage model for composite laminates used for low-velocity impact*

Wei GUO (郭　卫)[1], Pu XUE (薛　璞)[1], Jun YANG (杨　军)[2]

(1. School of Aeronautics, Northwest Polytechnical University, Xi'an 710072, P. R. China;
2. Chengdu Aircraft Design and Research Institute, Chengdu 610041, P. R. China)

Abstract In order to effectively describe the progressively intralaminar and interlaminar damage for composite laminates, a three dimensional progressive damage model for composite laminates to be used for low-velocity impact is presented. Being applied to three-dimensional (3D) solid elements and cohesive elements, the nonlinear damage model can be used to analyze the dynamic performance of composite structure and its failure behavior. For the intralaminar damage, as a function of the energy release rate, the damage model in an exponential function can describe progressive development of the damage. For the interlaminar damage, the damage evolution is described by the framework of the continuum mechanics through cohesive elements. Coding the user subroutine VUMAT of the finite element software ABAQUS/Explicit, the model is applied to an example, i.e., carbon fiber reinforced epoxy composite laminates under low-velocity impact. It is shown that the prediction of damage and deformation agrees well with the experimental results.

Key words composite laminate, progressive damage, delamination, energy release rate, low-velocity impact

Chinese Library Classification O346.5
2010 Mathematics Subject Classification 74A45

1 Introduction

As well known, composite laminates are susceptible to the low-velocity transverse impact. The damage from the impact load is one of the major design concerns for aeronautical composite structures. It has been shown that the low-velocity transverse impact could cause various damages, such as matrix cracks, delamination, and fiber breakage. Such damages are very difficult to be detected by naked eyes, but can cause significant reduction in the strength and stiffness of the materials. Hence, it is important to precisely predict the damage and its development in the laminates[1].

Virtual mechanical testing by means of numerical simulation of finite element software to analyze the impact damage resistance and the corresponding residual strength of a structure is of great interest and complexity. To predict the damage evolution in composite laminates under the low-velocity impact, extensive investigations were carried out, and some analytical models were proposed. Tan[2] proposed a progressive damage model based on the shell element. However, it cannot describe the interlaminate effect. With the enhancement of computing

* Received Jan. 7, 2013 / Revised Feb. 16, 2013
Project supported by the National Natural Science Foundation of China (No. 11072202)
Corresponding author Pu XUE, Professor, Ph. D., E-mail: p.xue@nwpu.edu.cn

capability, some researchers began use the three-dimensional (3D) solid element to improve the solution accuracy. After obtain the stress distribution of a structure, damage states need to be judged according to the failure criterion, and material properties need to be described as degradation. Chang[3] assumed that elastic constants of the material reduced to zero when studying the laminate strength of T300/976 composite laminates, that means the laminates could not continue to carry load once the failure occurred. It is obviously inconsistent with what is observed in the experiment. Camanho and Dávila[4] extended Chang's model[3] and proposed that the elastic constants of materials reduced to a constants instead of zero, when they analyzed the tensile strength of T300/914 composite laminates. It was better in describing the material degradation. However, a large amount of tests would be conducted to determine the coefficient in their model. In addition, the sudden reduction of the elastic constants may cause stiffness matrix singular in a numerical simulation. In order to solve these problems, some researchers presented the damage evolution in a continuous function based on the continuous damage mechanics, eventually describe the material stiffness matrix degradation. However, the implementation of the stress-softening or strain-softening constitutive model results in mesh-dependent results, i.e., the solution is non-objective with respect to the mesh refinement, and the computed energy dissipated decreases with the reduction of the element[5]. Zhang and Zhu[6] presented a strain failure criterion based on the Hashin criterion while studying the behavior of composite laminates under the low-velocity impact. However, their damage evolution rule did not include the energy dissipated and characteristic length, resulting that their prediction on the delamination area was larger than the experiment observation. Due to the complexity of impact response of the composite laminates, the damage and its evolution are still under investigation.

This study establishes a progressive damage model for composite laminates to be used for low-velocity impact, which is applied to a 3D solid element and cohesive elements to implement effectively analysis of intralaminar and interlaminar failure behavior for composite laminates. The proposed damage model is applied to analyze the composite panel under transverse impact using finite element software ABAQUS/Explicit with user subroutine VUMAT. The composite panel considered is carbon fiber reinforced epoxy composite laminates under a low-velocity impact.

2 Nonlinear progressive damage model for composite laminates

2.1 Intralaminar progressive damage model

2.1.1 Material damage constitutive model

Using the damage variable in the framework of Continuum Damage Mechanics to describe the material damage is an effective way. The 3D material damage constitutive model for orthotropic fiber reinforced composite laminates is

$$\sigma = C(d)\varepsilon, \tag{1}$$

where σ and ε are the effective Cauchy stress and Cauchy strain, respectively, while $C(d)$ is the stiffness matrix, which varies with the damage state.

A second-order symmetric tensor can be used to describe the damage state for the orthotropic fiber reinforced composite lamina. The first principal material direction is chosen to coincide with the longitudinal direction, and the second principal material direction is chosen to coincide with the transverse direction. The global damage variable is represented by d_{f} associated with the fiber failure, and d_{m} for the matrix failure. These global damage variables[7] are defined below,

$$d_{\mathrm{f}} = 1 - (1 - d_{\mathrm{ft}})(1 - d_{\mathrm{fc}}), \tag{2}$$

$$d_{\mathrm{m}} = 1 - (1 - d_{\mathrm{mt}})(1 - d_{\mathrm{mc}}), \tag{3}$$

where d_{ft}, d_{fc}, d_{mt}, and d_{mc} are the variables associated with fiber tensile, compression failure modes, matrix tensile, and compression failure modes, respectively. These damage variables are in the range [0,1], where $d = 0$ is corresponding to no damage, and $d = 1$ is corresponding to complete damage.

When material points fail, the stiffness matrix can be reduced as follows:

$$C_{11} = (1 - d_{\mathrm{f}})C_{11}^{0}, \tag{4}$$

$$C_{22} = (1 - d_{\mathrm{f}})(1 - d_{\mathrm{m}})C_{22}^{0}, \tag{5}$$

$$C_{33} = (1 - d_{\mathrm{f}})(1 - d_{\mathrm{m}})C_{33}^{0}, \tag{6}$$

$$C_{12} = (1 - d_{\mathrm{f}})(1 - d_{\mathrm{m}})C_{12}^{0}, \tag{7}$$

$$C_{23} = (1 - d_{\mathrm{f}})(1 - d_{\mathrm{m}})C_{23}^{0}, \tag{8}$$

$$C_{13} = (1 - d_{\mathrm{f}})(1 - d_{\mathrm{m}})C_{13}^{0}, \tag{9}$$

$$G_{12} = (1 - d_{\mathrm{f}})(1 - s_{\mathrm{mt}}d_{\mathrm{mt}})(1 - s_{\mathrm{mc}}d_{\mathrm{mc}})G_{12}^{0}, \tag{10}$$

$$G_{23} = (1 - d_{\mathrm{f}})(1 - s_{\mathrm{mt}}d_{\mathrm{mt}})(1 - s_{\mathrm{mc}}d_{\mathrm{mc}})G_{23}^{0}, \tag{11}$$

$$G_{13} = (1 - d_{\mathrm{f}})(1 - s_{\mathrm{mt}}d_{\mathrm{mt}})(1 - s_{\mathrm{mc}}d_{\mathrm{mc}})G_{13}^{0}, \tag{12}$$

where superscript "0" stands for the undamaged state. The coefficients s_{mt} and s_{mc} are introduced to shear stiffness loss due to the matrix failure under loading, which can be determined by experiments[7].

2.1.2 Failure criteria

The Hashin failure criteria[8] includes fiber tensile, fiber compression, matrix tensile failure, and matrix compression failure. Each failure can be described by a corresponding equivalent stress e_i, where i may be ft, fc, mt, and mc, named failure mode index. When the value of the failure mode index achieve to 1, the material at this point is regarded as failure. Four equivalent stresses under different failure modes can be defined and the failure criteria can be described as follows[9].

(i) For fiber tension failure,

$$e_{\mathrm{ft}} = \left(\frac{\sigma_1}{X_{\mathrm{t}}}\right)^2 \geqslant 1, \quad \sigma_1 \geqslant 0. \tag{13}$$

(ii) For fiber compression failure,

$$e_{\mathrm{fc}} = \left(\frac{\sigma_1}{X_{\mathrm{c}}}\right)^2 \geqslant 1, \quad \sigma_1 < 0. \tag{14}$$

(iii) For matrix tension failure,

$$e_{\mathrm{mt}} = \frac{(\sigma_{22} + \sigma_{33})^2}{Y_{\mathrm{t}}^2} + \frac{\sigma_{23}^2 - \sigma_{22}\sigma_{33}}{S_{23}^2} + \left(\frac{\sigma_{12}}{S_{12}}\right)^2 + \left(\frac{\sigma_{13}}{S_{13}}\right)^2 \geqslant 1, \quad (\sigma_{22} + \sigma_{33}) \geqslant 0. \tag{15}$$

(v) For matrix compression failure,

$$\begin{aligned} e_{\mathrm{mc}} =& \frac{1}{Y_{\mathrm{c}}}\left(\left(\frac{Y_{\mathrm{c}}}{2S_{23}}\right)^2 - 1\right)(\sigma_{22} + \sigma_{33}) + \frac{(\sigma_{22} + \sigma_{33})^2}{4S_{23}^2} \\ &+ \frac{\sigma_{23}^2 - \sigma_{22}\sigma_{33}}{S_{23}^2} + \left(\frac{\sigma_{12}}{S_{12}}\right)^2 + \left(\frac{\sigma_{13}}{S_{13}}\right)^2 \geqslant 1, \quad (\sigma_{22} + \sigma_{33}) < 0, \end{aligned} \tag{16}$$

where σ_1 is normal stress, σ_{ij} is shear stress, and X_{t}, X_{c}, Y_{t}, Y_{c}, S_{12}, S_{23}, and S_{13} are the longitudinal tensile strength, the longitudinal compressive strength, the transverse tensile strength, the transverse compressive strength, the longitudinal shear strength, and the two transverse shear strengths, respectively.

2.1.3 Material degradation

If failure is detected in a material point of the composite laminates, its material properties have to be adjusted according to a material degradation model. The mode of the degradation can be one of the three modes: instantaneous reduce to zero, reduce to a constant stress, and gradually reduce in a given path[10], as shown in Fig. 1.

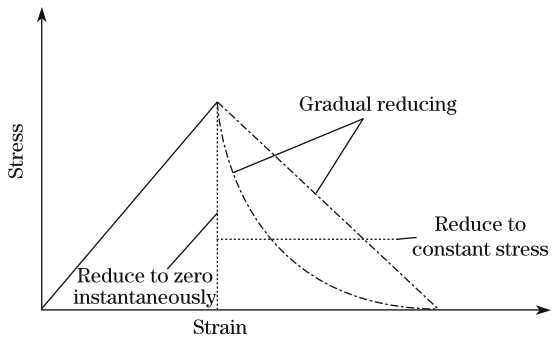

Fig. 1 Properties degradation behavior in damage composite laminates

In this study, an exponential function of energies dissipated by damage is established. It can not only describe progressive development of the damages, but also avoid the stiffness matrix singularity due to the material stiffness abrupt variation. When implementation for a stress-softening constitutive model, the results are mesh-dependent, e.g., the solution is non-objective with respect to the mesh refinement, and the computed energy dissipated decreases with the reduction of the element dimension. Thus, the energy dissipation and characteristic length are introduced into the damage evolution law to reduce the mesh sensitivity[11]. The damage variables are defined as follows[12]:

$$d_{\mathrm{ft}} = 1 - \left(\frac{1}{e_{\mathrm{ft}}}\right)\mathrm{e}^{(-C_{11}\varepsilon_{11}^{\mathrm{ft}}\varepsilon_{11}^{\mathrm{ft}}(e_{\mathrm{ft}}-1)L_{\mathrm{c}}/G_{\mathrm{ft}})}, \tag{17}$$

$$d_{\mathrm{fc}} = 1 - \left(\frac{1}{e_{\mathrm{fc}}}\right)\mathrm{e}^{(-C_{11}\varepsilon_{11}^{\mathrm{fc}}\varepsilon_{11}^{\mathrm{fc}}(e_{\mathrm{fc}}-1)L_{\mathrm{c}}/G_{\mathrm{fc}})}, \tag{18}$$

$$d_{\mathrm{mt}} = 1 - \left(\frac{1}{e_{\mathrm{mt}}}\right)\mathrm{e}^{(-C_{22}\varepsilon_{22}^{\mathrm{mt}}\varepsilon_{22}^{\mathrm{mt}}(e_{\mathrm{mt}}-1)L_{\mathrm{c}}/G_{\mathrm{mt}})}, \tag{19}$$

$$d_{\mathrm{mc}} = 1 - \left(\frac{1}{e_{\mathrm{mc}}}\right)\mathrm{e}^{(-C_{22}\varepsilon_{22}^{\mathrm{mc}}\varepsilon_{22}^{\mathrm{mc}}(e_{\mathrm{mc}}-1)L_{\mathrm{c}}/G_{\mathrm{mc}})}, \tag{20}$$

where G_{ft}, G_{fc}, G_{mt}, and G_{mc} are energies dissipated by damage for fiber tension, fiber compression, matrix tension, and matrix compression failure modes, respectively. L_{c} is the characteristic length.

2.1.4 Material properties update

The material properties updating using the ABAQUS subroutine in VUMAT can be illustrated in Fig. 2.

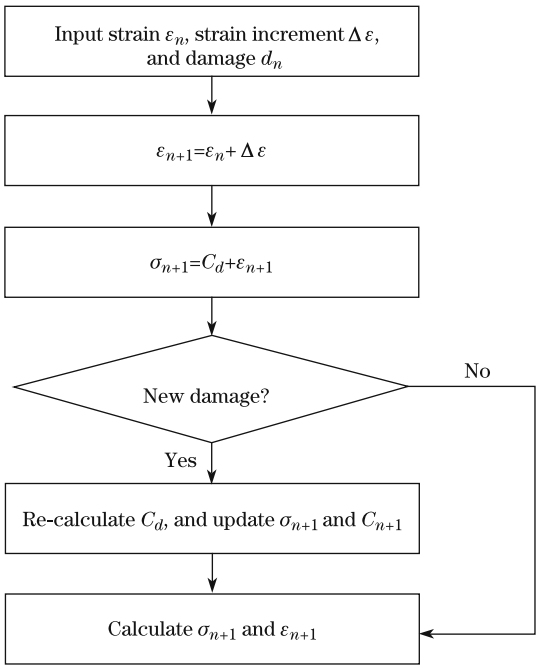

Fig. 2 Flow chart of VUMAT

2.2 Interlaminar progressive damage model

Interlaminar damage (delamination) is the dominate failure mode in the composite laminates, especially under a low-velocity impact[13]. In ABAQUS[14], the cohesive element can be able to capture delamination onset and growth under the mixed-mode loading condition. The nominal traction stress vector, $\boldsymbol{t}$, which consists of three components t_n, t_s, and t_t, can be calculated using the stiffness in Modes I, II, and III, and the opening and/or sliding displacements, $\boldsymbol{\delta}$, which also consists of three components δ_n, δ_s, and δ_t, as show below.

$$\boldsymbol{t} = \begin{pmatrix} t_\mathrm{n} \\ t_\mathrm{s} \\ t_\mathrm{t} \end{pmatrix} = \begin{pmatrix} k_\mathrm{n} & & \\ & k_\mathrm{s} & \\ & & k_\mathrm{t} \end{pmatrix} \begin{pmatrix} \delta_\mathrm{n} \\ \delta_\mathrm{s} \\ \delta_\mathrm{t} \end{pmatrix} = \boldsymbol{K}\boldsymbol{\delta}, \tag{21}$$

where k_n, k_s, and k_t are the cohesive element normal stiffness and two shear stiffness, respectively.

Camanho and Dávila[4] introduced an interface element between each ply of the composite laminates, and proposed a stress failure criterion to predict damage initiation,

$$\left(\frac{\langle\sigma_\mathrm{n}\rangle}{N}\right)^2 + \left(\frac{\sigma_\mathrm{s}}{S}\right)^2 + \left(\frac{\sigma_\mathrm{t}}{T}\right)^2 = 1, \tag{22}$$

where $\langle\cdot\rangle$ is the Macaulay bracket defined as $\langle x\rangle = \frac{1}{2}(x+|x|)$. σ_n denotes the traction normal stress, and σ_s and σ_t denote shear stresses, while N, S, and T are defined as the corresponding interlaminar normal and two shear strengths.

Once the damage occurs, the material stiffness is needed degradation in terms of a damage variable d. Its values range from zero when damage onsets to 1 when complete delamination occurred. The failure criterion to predict delamination propagation under the mixed-mode loading is expressed in terms of the energy release rates associated with modes I, II, and III, and the typical traction separation is shown in Fig. 3. For a linear softening process, the damage variable d for the delamination evolution is defined as follows:

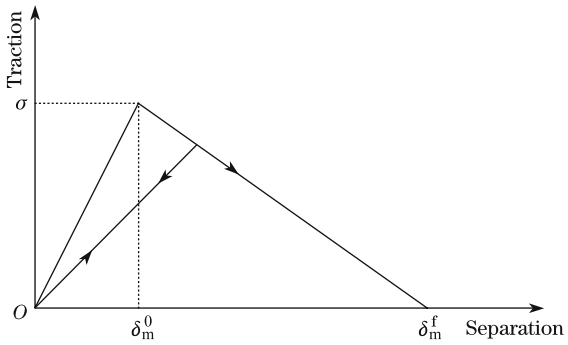

Fig. 3 Typical traction separation

$$d=\frac{\delta_{\mathrm{m}}^{\mathrm{f}}(\delta_{\mathrm{m}}^{\max}-\delta_{\mathrm{m}}^{0})}{\delta_{\mathrm{m}}^{\max}(\delta_{\mathrm{m}}^{\mathrm{f}}-\delta_{\mathrm{m}}^{0})}, \tag{23}$$

where $\delta_{\mathrm{m}}^{\max}$ is defined as the maximum relative displacement,

$$\delta_{\mathrm{m}}=\sqrt{\langle\delta_{\mathrm{n}}\rangle^{2}+\delta_{\mathrm{s}}^{2}+\delta_{\mathrm{t}}^{2}}. \tag{24}$$

In Eq. (23), $\delta_{\mathrm{m}}^{\mathrm{f}}$ is the mixed-mode displacement at complete failure, and δ_{m}^{0} is the effective displacement at damage onset. A mixed-mode criterion proposed by Benzeggaph-Kenane is used here (BK criterion[15]). This criterion is expressed as a function of mode I and mode II fracture toughness (G) and a parameter η obtained from mixed-mode bending tests at different mode ratios,

$$\delta_{\mathrm{m}}^{\mathrm{f}}=\begin{cases}\dfrac{2}{K\delta_{\mathrm{m}}^{0}}\Big(G_{\mathrm{IC}}+(G_{\mathrm{IIC}}-G_{\mathrm{IC}})\Big(\dfrac{\beta^{2}}{1+\beta^{2}}\Big)^{\eta}\Big), & \delta_{\mathrm{n}}>0\\ \sqrt{(\delta_{\mathrm{s}}^{\mathrm{f}})^{2}+(\delta_{\mathrm{t}}^{\mathrm{f}})^{2}}, & \delta_{\mathrm{n}}\leqslant 0\end{cases} \tag{25}$$

where β is the mode mixity ratio.

3 Validation of proposed model

3.1 Geometrical parameter and finite model

Carbon-epoxy composite laminates considered in this section is a clamped circular panel with diameter of 50 mm. It is impacted with a hemispherical impactor with diameter of 25 mm and weight of 2.428 kg. The composite laminates have the stacking sequence of $(0_4/90_4)$, and the mechanical properties are listed in Table 1[16–17].

Table 1 Mechanical properties of unidirectional carbon-epoxy material

E_{11}/GPa	$E_{22}=E_{33}$/GPa	$\upsilon_{12}=\upsilon_{13}$	υ_{23}	$G_{12}=G_{13}$/GPa	G_{23}/GPa
109.34	88.2	0.342	0.52	4.32	3.2
X_{c}/MPa	Y_{t}/MPa	Y_{c}/MPa	S_{12}/MPa	S_{23}/MPa	S_{13}/MPa
1 132	59	211	54	54	54

The finite element model is established (see Fig. 4). There are four layers of solid elements using brick elements of 8-node linear, reduced integration with hourglass control, named C3D8R,

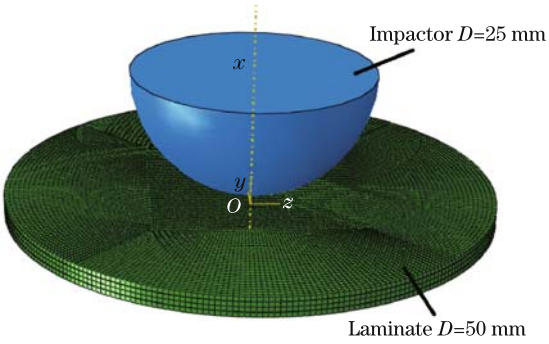

Fig. 4 Finite element model

and two cohesive elements named COH3D8 between different oriented layers, considering delamination mostly appears at interface with different stacking direction from the experimental observation. The impactor is defined as a rigid body and modeled by a lumped mass. Tables 2 and 3 list the intralaminar strength and toughness properties and the interlaminar toughness properties, respectively.

Table 2 Interlaminar strength and fracture toughness[16]

N/MPa	S/MPa	T/MPa	$G_{\mathrm{IC}}/(\mathrm{J}\cdot\mathrm{m}^{-2})$	$G_{\mathrm{IIC}}/(\mathrm{J}\cdot\mathrm{m}^{-2})$	$G_{\mathrm{IIIC}}/(\mathrm{J}\cdot\mathrm{m}^{-2})$
59	59	59	306	632	817

Table 3 Interlaminar toughness properties[18–19]

$G_{\mathrm{ft}}/(\mathrm{J}\cdot\mathrm{m}^{-2})$	$G_{\mathrm{fc}}/(\mathrm{J}\cdot\mathrm{m}^{-2})$	$G_{\mathrm{mt}}/(\mathrm{J}\cdot\mathrm{m}^{-2})$	$G_{\mathrm{mc}}/(\mathrm{J}\cdot\mathrm{m}^{-2})$
81 500	106 300	306	1 050.2

The general contact algorithm which defines a linear pressure-overclosure relationship is used to model the potential contact between the impactor and the panel. In addition, the coulomb friction model which relates the maximum frictional stress $\tau_{\max}$ to the normal contact pressure between the contacting bodies P, which can be defined as $\tau_{\max} = \mu P$. The friction coefficient[13] for contacts between the impact and the panel is taken as $\mu = 0.3$.

3.2 Results and discussion

To compare our prediction with the impact experimental data[16–17], the impact velocities of 1.13 m/s, 1.20 m/s, and 1.24 m/s are chosen, respectively. Figure 5 shows the impact force history and energy dissipated by damage history (ALLDMD) under the impact velocity of 1.13 m/s. It can be seen that the impact process can be divided into 3 stages.

(i) Stage I From point 0 to point P_1, there is no interlaminar damage in this stage, and the value of ALLDMD is almost zero. The impact force grows rapidly. In addition, the energy at point P_1 can be thought of as the impact damage threshold[13,20].

(ii) Stage II From point P_1 to P_2, the impact force reaches its maximum value at the point P_2. In this stage, the delamination for the back layer grows, and expands rapidly, correspondingly the value of ALLDMD increases rapidly, and the growth rate of impact force slows down significantly. Until the speed of the impactor decreases to zero, all the kinetic energy consumes completely.

(iii) Stage III From point P_2 to P_3, the impact force begins to unload, but the value of ALLDMD keeps a constant, which means the damage does not develop further.

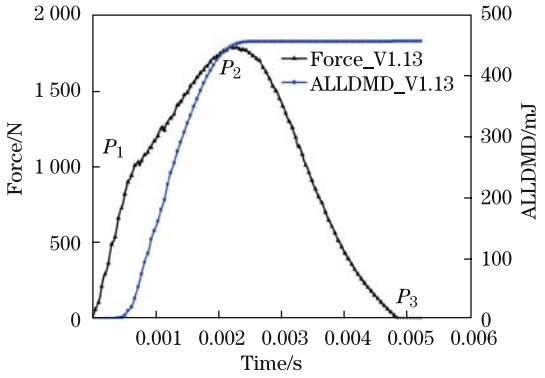

Fig. 5 Impact force and energy dissipated by damage for impact velocity of 1.13 m/s

After impact, the main failure modes observed are matrix cracking and delamination at the back layer, as well as the matrix cracking at the top layer, and no fiber damage occurred, which is consistent with the experiment. Figure 6 shows the damage of the matrix cracking and delamination at the back layer. Due to the stress along the fiber direction decreases more quickly, eventually makes the matrix cracking is along the fiber direction, and the closer to the back of the composite laminates, the more serious of the damage. The delaminated area mainly in the shape of double leaf, i.e., peanut, shape with the spindle along the fiber direction at the bottom layer, which is consistent with the experimental observation[16–17], as shown in Fig. 7.

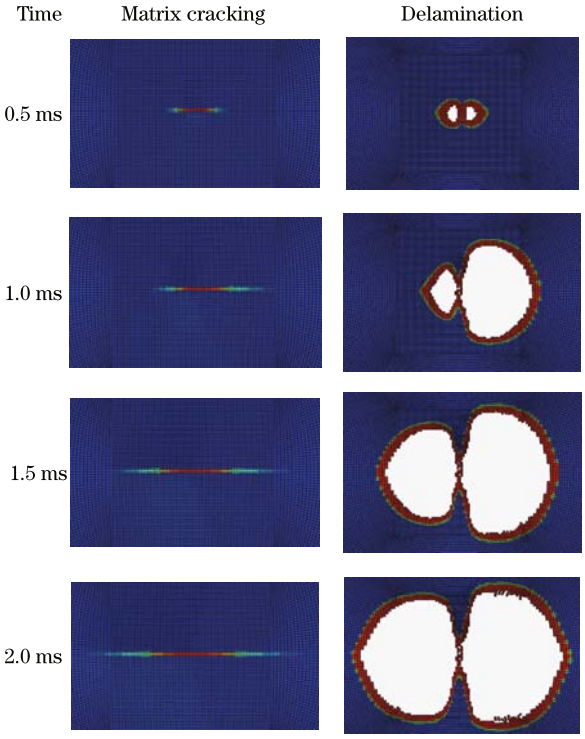

Fig. 6 Matrix cracking and delamination in back layer under impact velocity of 1.13 m/s

Impact force for the three different impact velocities 1.13 m/s, 1.20 m/s, and 1.24 m/s are shown in Fig. 8. It can be seen that the bigger the impact velocity is, the larger the peak force is. The forces at the points P_1 are coincident and can be regarded as the impact damage threshold[13,20].

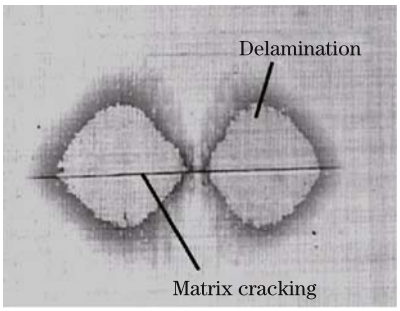

Fig. 7 Experiment result[16–17] under impact velocity of 1.13 m/s

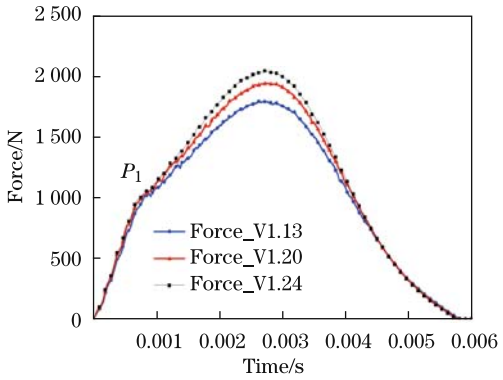

Fig. 8 Impact forces for three different impact velocities

A comparison between the numerical results and the experiments is presented in Table 4. The maximum length and width of the delamination area and the crack length are compared. The reasonable agreement can be seen except for that under velocity 1.24 m/s. The error may come from the boundary difference between the experimental and numerical simulation.

Table 4 Experimental and numerical results for delaminations and crack sizes

Impact velocity /(m·s^{-1})	F_e /KN	F_p /KN	Error (F) /%	S_e /mm^2	S_p /mm^2	Error (S) /%	L_e /mm	L_p /mm	Error (L) /%
1.20	1.98	1.95	–1.8	392	420	7.14	37	33.6	–9.2
1.24	2.24	2.05	–8.7	743	534	–27.4	46	35.7	–22.4

In Table 4, F, S, and L are the peak force, the delamination area, and the length of matrix cracking, respectively. Subscript e stands for the experimental result, and subscript p stands for the numerically predicted result.

4 Conclusions

Based on the theory of continuous damage mechanics, a three dimensional progressive damage model for composite laminates to be used for low-velocity impact is presented. The prediction for damage and deformation agrees well with the experimental results. The following conclusions are drawn:

(i) For the intralaminar damage, the damage model is described as an exponential function of energy release rate. It can not only describe progressive development of the damages, but also avoid the stiffness matrix singularity resulting from the material stiffness abrupt reduction. The model also introduces the characteristic length to reduce the mesh grid dependence of the simulation results.

(ii) For the interlaminar damage, damage evolution is described by combining the stress failure criterion and the energy release rate criterion through cohesive elements.

(iii) Under low-velocity impact, matrix cracking and delamination are firstly detected. Fiber fracture occurs only when the large impact energy is applied. The fiber fracture occurs later than that of the matrix cracking. The cracking in most cases is along the fiber direction. The closer to the back of the panel, the more serious of the damage. The delaminated area is in the shape of double leaf with the spindle along the fiber direction at the bottom layer, which is consistent with the experimental observation.

References

[1] Li, C. F. and Hu, N. Low-velocity impact-induced damage of continuous fiber-reinforced composite laminates, part I: an FEM numerical model. *Composites Part A*: *Applied Science and Manufacturing*, **33**(8), 1055–1062 (2002)

[2] Tan, S. C. A progressive failure model for composite laminates containing openings. *Journal of Composite Materials*, **25**, 556–577 (1991)

[3] Chang, F. C. K. A progressive damage model for laminated composites containing stress concentrations. *Journal of Composite Materials*, **21**, 834–855 (1987)

[4] Camanho, P. P. and Dávila, C. G. *Mixed-Mode Decohesion Finite Elements for the Simulation of Delamination in Composite Material*, NASA/TM-2002-211737, 1–37 (2002)

[5] Cheng, X. Q. and Li, Z. N. Damage progressive model of compression of composite laminates after low-velocity impact. *Appl. Math. Mech. -Engl. Ed.*, **26**(5), 618–626 (2005) DOI 10.1007/BF 02466336

[6] Zhang, Y. and Zhu, P. Finite element analysis of low-velocity impact damage in composite laminated plates. *Materials & Design*, **27**(6), 513–519 (2006)

[7] Pederson, J. *Finite Element Analysis of Carbon Fiber Composite Ripping Using ABAQUS*, Clemson University, Clemson (2006)

[8] Hahin, Z. Failure criteria for unidirectional fiber composites. *Journal of Applied Mechanics*, **47**(2), 329–335 (1980)

[9] Wang, S. and Wu, L. Low-velocity impact and residual tensile strength analysis to carbon fiber composite laminates. *Materials & Design*, **31**, 118–125 (2010)

[10] David, W. *Progressive Failure Analysis Methodology for Laminated Composite Structures*, NASA/TP-1999-209107 (1999)

[11] Lapczyk, I. and Hurtado, J. A. Progressive damage modeling in fiber-reinforced materials. *Composites Part A*: *Applied Science and Manufacturing*, **38**(11), 2333–2341 (2007)

[12] Linde, P. and Pleitner, J. Modelling and simulation of fibre metal laminates. *ABAQUS Users' Conference*, Boston, USA, 421–439 (2004)

[13] Gonzáez, E. V., Maimí, P., Camanbo, P. P., Turon, A., and Mayugo, J. A. Simulation of drop-weight impact and compression after impact tests on composite laminates. *Composite Structures*, **94**(11), 3364–3378 (2012)

[14] Dassault Systems. *ABAQUS Version A*. 6.8-1 *User Documentation*, Velizy-Villacoublay (2008)

[15] Benzeggagh, M. L. and Kenane, M. Measurement of mixed-mode delamination fracture toughness of unidirectional glass/epoxy composites with mixed-mode bending apparatus. *Composites Science and Technology*, **56**(4), 439–449 (1996)

[16] De Moura, M. F. S. F. and Gonļves, J. P. M. Modelling the interaction between matrix cracking and delamination in carbon-epoxy laminates under low-velocity impact. *Composites Science and Technology*, **64**(7-8), 1021–1027 (2004)

[17] De Moura, M. F. S. F. and Marques, A. T. Prediction of low-velocity impact damage in carbon–epoxy laminates. *Composites Part A*: *Applied Science and Manufacturing*, **33**(4), 361–368 (2002)

[18] Lopes, C. S. and Camanho, P. P. Low-velocity impact damage on dispersed stacking sequence laminates, part II: numerical simulations. *Composites Science and Technology*, **69**(7), 937–947 (2009)

[19] Turon, A. and Camanho, P. P. Accurate simulation of delamination growth under mixed-mode loading using cohesive elements: definition of interlaminar strengths and elastic stiffness. *Composite Structures*, **92**(8), 1857–1864 (2010)

[20] Gonz, A., Lez, E. V., and Maim, I. P. Effects of ply clustering in laminated composite plates under low-velocity impact loading. *Composites Science and Technology*, **71**(6), 805–817 (2011)